

021 **ACTIVE SHAPE MODELING TECHNIQUES IN OPHTHALMOLOGY: AUTOMATIC SEGMENTATION OF THE EYE IN MAGNETIC RESONANCE IMAGING OF CHILDREN**C. Ciller^{1,2,3}, S.I. De Zanet^{2,4}, A. Pica⁵, P. Maeder¹, F. L. Munier⁶, J. H. Kowal^{2,4}, M. Bach Cuadra^{3,1,7}

- 1 Department of Radiology, University Hospital Center (CHUV) & UNIL, Lausanne, Switzerland,
- 2 Ophthalmic Technology Group, ARTORG Center, University of Bern (UniBe), Bern, Switzerland,
- 3 Center for Biomedical Imaging (CIBM), University of Lausanne (UNIL), Lausanne, Switzerland,
- 4 Department of Ophthalmology, Inselspital, Bern University Hospital, Bern, Switzerland.
- 5 Department of Radiation Oncology, Inselspital, Bern Univ. Hosp. & Univ. of Bern (UniBe), Switzerland,
- 6 Unit of Pediatric Ocular Oncology, Jules-Gonin Eye Hosp., UNIL, Lausanne, Switzerland,
- 7 Signal Processing Lab. (LTS5), Ecole Polytechnique Fédérale de Lausanne (EPFL), Switzerland,

Background: Delineation of ocular anatomy in 3D imaging involves a big challenge for ophthalmologists, mostly when developing the treatment planning for ocular diseases. Magnetic resonance imaging (MRI) is used today in clinical practice as a complementary source of information, together with fundus imaging or ultrasound, in diagnosis and treatment planning for retinoblastoma in children. Here we present a novel 3D statistical Active Shape Model (ASM)[1] to automatically segment the eye anatomy in the MRI.

Aims: To develop an Active Shape Model (ASM) based on 3D MRI for precise children eye segmentation.

Methods: Our data set is composed of 12 healthy eyes from children aged 3.2 ± 1.7 years old. Imaging was performed a 3T Siemens TimTrio machine (Siemens, Erlangen, Germany), with a 32-channel surface head coil attached. The images are T_1 -Weighted GE VIBE (TE/TR, 3.91/20 ms). The Dataset has images which were acquired at two different spatial resolutions of $0.416 \times 0.416 \times 0.399$ mm and $0.48 \times 0.48 \times 0.5$ mm. All the volumes were resampled to a common space $0.416 \times 0.416 \times 0.399$ mm for constructing the model.

The eye model comprises the regions of the lens, the vitreous humor, the sclera and the cornea. Manual delineations were done for all subjects and structures. They were corrected for all orthogonal planes by a senior radiation oncologist. The model construction is done by combining all the surfaces extracted from the manual delineation, generating a shape variation model, and coupling it with the intensity information to build the ASM as suggested in [2,3]. The segmentation of a subject works as follows. We first automatically detect the position of the center of the eye, the lens and the optic nerve, using the algorithm proposed in [4] for aligning the model. Afterwards, we proceed to do the fitting by minimizing the Mahalanobis distance between the ASM and the subject until convergence.

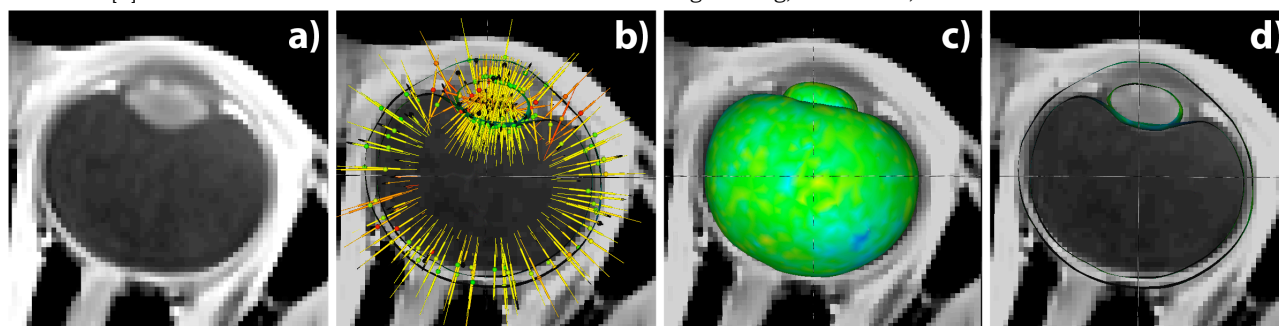
We quantitatively validate our segmentation method with a leave-one-out cross validation test. The resulting segmentation is assessed by the overlapping measure (Dice Similarity Coefficient, DSC) with the manual segmentation used as the ground truth (GT). Additionally, we provide a measure of the mean distance error of the given segmentation wrt. the GT for every region in the eye.

Results: Through the leave-one-out test for the ASM fitting, we obtain an average DSC of $96.68 \pm 1.24\%$ for the sclera and the cornea, a $95.88 \pm 1.73\%$ for the vitreous humor and $84.41 \pm 3.4\%$ for the lens. The mean overall distance error is 0.20 ± 0.09 mm for both the sclera and the cornea and the vitreous humor. For the lens we reach an average error of 0.21 ± 0.1 mm. The entire segmentation process takes in total 8 s.

Conclusions: We have shown a reliable and accurate segmentation tool that enables clinicians to automatically delineate the sclera, the cornea, the vitreous humor and the lens in MRI. This tool will contribute to reduce the time spent in the tedious task of eye shape delineation and will eventually help clinicians during ocular tumor treatment planning and diagnosis confirmation.

Acknowledgements: This work is supported by a grant from the Swiss Cancer League. This work is also supported by the Centre d'Imagerie BioMédicale (CIBM) of the University of Lausanne (UNIL), the École Polytechnique Fédérale de Lausanne (EPFL), the University of Geneva (UniGe), the Centre Hospitalier Universitaire Vaudois (CHUV), the Hôpitaux Universitaires de Genève (HUG), the University of Bern (UniBe) and the Leenaards and the Jeantet Foundations.

References: [1] Cootes, et al. Computer Vision and Image Understanding, Vol. 61, No. 1, 38-59, 1995.
 [2] Rügsegger et al., Int J. Radiation Oncol. Biol. Phys, Vol. 84, No 4, 2012.
 [3] Frangi et al. IEEE Transactions on Medical Imaging, Vol. 21, n 9, 2002.
 [4] De Zanet et al. IEEE Transactions on Biomedical Engineering, Submitted, 2014.



Figures: (a) Pre-processed MRI. b) Model Initialization c) Automatic Fitting. d) Final Segmentation.